

# Poly(3-decylthiophene) Radical Anions and Cations in Solution: Single and Multiple Polarons and Their Delocalization Lengths in Conjugated Polymers

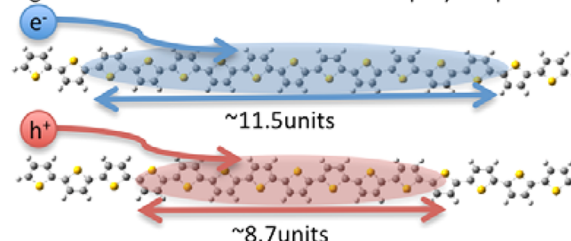
Norihiko Takeda and John R. Miller\*

Chemistry Department, Brookhaven National Laboratory, Upton, New York 11973-5000, United States

**S** Supporting Information

**ABSTRACT:** Optical absorption spectra of anions and cations of poly(3-decylthiophene) (P3DT) in solution were identified as single polarons. Pulse radiolysis of P3DT in THF determined the spatial extent of one negative polaron to be  $\sim 11.5$  thiophene units by observing transient absorption of  $\text{P3DT}^{\bullet-}$  radical ions, which are principally free ions, at 850 nm with  $\epsilon = (7.25 \pm 0.47) \times 10^4 \text{ M}^{-1} \text{ cm}^{-1}$  and bleaching of the neutral absorption band at 450 nm.  $\text{P3DT}^{\bullet-}$  was formed in a combination of diffusive reactions and fast “step” processes. Similarly, a positive polaron of P3DT was estimated to delocalize over  $\sim 8.7$  thiophene units by pulse radiolysis in chloroform. Chemical reduction by sodium and oxidation by  $\text{FeCl}_3$  injected multiple charges into a single P3DT chain while showing absorption spectra in the early stages of reaction resembling those observed by pulse radiolysis. The results indicated that multiple polarons exist in a single chain of P3DT before coalescing into bipolarons or transforming into other forms of polaron.

## Charge attachment and delocalization in polythiophene



## INTRODUCTION

Polythiophene (pT) is a representative conducting polymer that can be doped with either negative (n-doping) or positive (p-doping) charges.<sup>1–3</sup> Along with the fullerene [6,6]-phenyl- $\text{C}_{61}$ -butyric acid methyl ester (PCBM), it is the basic constituent of organic photovoltaic cells having almost 5% efficiency.<sup>4</sup> In such cells, electron transfer injects holes into pT/PCBM films. Experiments and theory have sought to understand the nature of charges in pT. Experiments often involve doping of pT and related polymers chemically or electrochemically, with multiple charges injected per one polymer chain. The chemical structures of poly- and oligothiophenes are represented by a thiophene unit and a number of conjugated repeat units  $n$  in Figure 1. Charge injection into nondegenerate  $\pi$ -conjugated polymers forms polarons or bipolarons, which are bound charged states spread over a few or several units in which the geometries are distorted from the neutral states. Theory<sup>5–16</sup> describes polarons as singly charged radical ions, containing a singly occupied molecular orbital (SOMO) between the highest occupied molecular orbital (HOMO) and lowest unoccupied molecular orbital (LUMO) (Figure 1). Observations of microwave conductivity<sup>17–27</sup> are best understood in terms of polarons. Injection of an electron (n-doping) causes the singly occupied state (SOMO) to move downward from the energy of the unoccupied LUMO, whereas doubly occupied states move upward. Accordingly, new optical absorption bands are expected to appear at energies below the HOMO–LUMO transition of neutral molecules. The two bands (P1 and P2) observed in the near-infrared (NIR) and visible (vis) regions

can be assigned mainly to SOMO-to-LUMO and HOMO-to-SOMO transitions, respectively. A third band (P3) is also expected [i.e., (HOMO – 1)-to-SOMO] that would overlap with the neutral HOMO-to-LUMO transition. Likewise, injection of a positive charge (p-doping) causes two bands in the vis–NIR region mainly due to SOMO-to-LUMO and HOMO-to-SOMO transitions. Further addition of an electron to the SOMO of a negative polaron or extraction of an electron from the SOMO of a positive polaron would produce a doubly charged closed-shell ion called a bipolaron.

Bipolarons are produced if two neighboring polarons with like charges overcome their electrostatic repulsion, possibly with the aid of counterions utilized in the doping, and share a geometrical distortion. Classically, charge doping of polythiophene had been thought to form bipolarons.<sup>1,8–10,28,29</sup> Observations that electron spin resonance signals increased and then decreased with doping of polythiophene were thought to indicate that spinless bipolarons were more stable than polarons.<sup>10,28</sup> On the other hand, more recent works have reported that two absorption bands are indicative of polarons and that they are the more stable form of localized charged states.<sup>11,30,31</sup> Although a growing number of works favor polarons as the more likely charge carriers,<sup>11,30,32,33</sup> the question of what form injected charges take remains unclear.

Knowing the nature of charge carriers is important for understanding the charge transport through these long

**Received:** September 27, 2012

**Revised:** November 14, 2012

**Published:** November 17, 2012

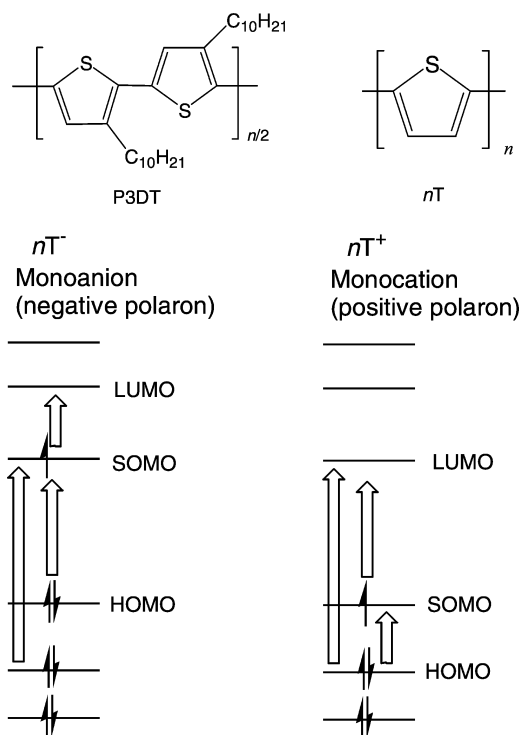


**Figure 1.** Chemical structures of P3DT and  $T_n$ s and energy diagrams for their polarons. Principal electronic transitions for new absorption bands in the NIR, visible, and UV regions (P1, P2, and P3, respectively) are indicated by arrows.

molecules. Greater electronic coupling between neighboring units tends to delocalize the charges, whereas geometry changes and ion pairing<sup>12–14</sup> created by doping tend to localize them. Usually, delocalization is partial, and the charge spreads out to become a polaron having a length determined by the competition between electronic coupling and geometric relaxation. Longer polarons lead to greater mobility. Charge hopping by thermal excitation is strongly correlated with the extent of energy gained by polaron formation.

The present study utilized both pulse radiolysis and chemical methods to investigate charged conducting polymers in solution. Together, these methods provide insight that is not otherwise available. Two characteristics of pulse-radiolysis experiments are important: (1) They produce single charges (polarons) definitively, and (2) they provide rapid injection with time-resolved detection by optical spectroscopy. We chose regioregular poly(3-decylthiophene) (P3DT, Figure 1) as a target compound that was dissolved in tetrahydrofuran (THF) and chloroform. Strong reducing agents (solvated electrons and sodium) and strong oxidizing agents (solvated radical cations and ferric chloride) were used to selectively attach charges to the molecules in appropriate solvents. Furthermore, the ability of pulse radiolysis to measure spectra of molecular ions at low concentrations enables the characterization of singly charged polymers in solution. Absorption coefficients of singly charged P3DT were determined, and their delocalization lengths were estimated by simultaneously observing bleaching of neutral bands and growth of polaron bands. Comparisons of chemically produced spectra with those observed by pulse radiolysis suggest the generation of multiple polarons in a single chain.

## EXPERIMENTAL SECTION

**Chemicals.** Regioregular poly(3-decylthiophene-2,5-diyl) (P3DT; Rieke Metal Inc., >98.5% head-to-tail)<sup>34</sup> was purchased from Aldrich and used as received. Gel permeation chromatography (GPC) measurements (Figure S1 in the Supporting Information) revealed a number-average molecular weight of  $M_n \approx 38000$  and a weight-average molecular weight of  $M_w \approx 120000$  (polydispersity index  $M_w/M_n \approx 3.2$ ). From the measured  $M_n$ , the average number of units was estimated to be  $n \approx 170$ . For P3DT, concentrations are expressed in terms of monomer-unit concentrations (formula weight 222.39) unless otherwise noted. Quaterthiophene (Aldrich),  $T_4$ , was purified by recrystallization from toluene followed by sublimation under a vacuum.<sup>35</sup> Biphenyl (Fischer) was either recrystallized four times from ethanol or zone-refined in ambient air. Tri-*p*-tolylamine (TTA; Aldrich, 97%) was recrystallized from absolute ethanol and sublimed under a vacuum. 2-Ethylanthraquinone (Aldrich, 97%) was zone-refined in ambient air. Solvents used for pulse-radiolysis experiments were purified as follows: Tetrahydrofuran (Aldrich, anhydrous, inhibitor-free) was distilled from sodium benzophenone ketyl and stored under argon. Chloroform (Aldrich, HPLC grade, stabilized with ethanol) was treated repeatedly with molecular sieve 5A and stored under argon. 1,2-Dichloroethane (DCE; Aldrich) was stored over molecular sieves 3A and 5A. Water was purified with a Milli-Q water purification system ( $18 \text{ M}\Omega \text{ cm}^{-1}$ ).

**Pulse Radiolysis.** Radiation of 9 MeV, <100 ps electron pulses (5–10 nC) and transient optical absorption measurements were performed at the Laser Electron Accelerator Facility (LEAF) at Brookhaven National Laboratory.<sup>36–38</sup> Probe light from a pulsed xenon arc lamp was wavelength-selected with interference filters (10- or 40-nm bandwidth) and recorded with photodiodes (Si for 400–1100 nm, Ge for 1000–1627 nm, and InGaAs for 1500–2500 nm) and a 1-GHz oscilloscope (Tektronix 680B). A biplanar phototube (Hamamatsu 1193u) was used when a faster time response was needed. An appropriate cutoff filter (432 or 587 nm) was inserted in front of the sample. Sample solutions were prepared under an argon atmosphere (in a glovebox) and sealed in fused-silica quartz cells equipped with Teflon screw caps (1-, 5-, or 20-mm path length). A Faraday cup monitored charges from each electron pulse and was used to normalize the dose among different shots. A deaerated aqueous solution of 1 M NaOH and 10 vol % methanol in Milli-Q water was used as a reference sample to compare day-to-day doses by measuring its hydrated electron absorption. Each pulse produced  $1 \pm 0.5 \mu\text{M}$  of solvated electrons; the fraction attached to molecules was determined within a kinetic model.<sup>33,39</sup> Measurements of molar absorption coefficients were calibrated against known values to account for day-to-day variations.

**UV–Vis–NIR Spectroscopy.** Stationary absorption spectra were recorded using a Cary 5 UV–vis–NIR spectrophotometer (Varian Instruments). Spectra of neutral (undoped) P3DT were measured in ambient air. Neutral P3DT showed a lowest energy electronic absorption peak corresponding to its HOMO–LUMO transition at 448 nm in THF. Peak absorbances of different concentrations between 0.2 and 1.6 mM obeyed Beer's law, and an absorption coefficient of  $\epsilon_{448} = 8.3 \times 10^3 \text{ M}^{-1} \text{ cm}^{-1}$  per repeat unit was obtained. Similar measurements in chloroform showed a peak at 451 nm and a corresponding absorption coefficient of  $\epsilon_{451} = 8.6 \times 10^3 \text{ M}^{-1} \text{ cm}^{-1}$ . In 1,2-dichloroethane (DCE), the absorption spectra of

P3DT showed several peaks at 520, 555, and 606 nm, and the band extended into the NIR region ( $\sim 1100$  nm). (In the Supporting Information, spectra are shown in Figures S2 and S3; Figure S4 compares poly- and oligothiophenes.) These observations suggest different secondary structures or the formation of aggregates, which is known to occur in polythiophenes.<sup>40</sup>

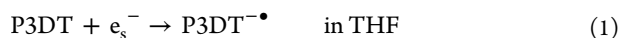
Chemical reductions of P3DT and  $T_4$  in THF were performed in a vacuum-sealed cell as follows: The four-way cell consisted of a 1-mm-path-length Infrasil cell (Starna Cells, Inc.) for optical measurements, a solution reservoir, a sodium film compartment that was separated by a glass filter, and a connection to a vacuum line. The sodium film was prepared by in situ distillation under a vacuum. Solutions of polymers or oligomers were prepared in the cell by vacuum transfer of THF from a reservoir containing NaK alloy. Absorption spectra in a 200–3300-nm range were measured before and after successive contacts with the sodium film.

Chemical oxidation of P3DT in chloroform was performed using anhydrous  $FeCl_3$  (Aldrich) as the oxidizing agent. The chloroform solution of P3DT prepared under argon in a 2-mm-path-length Infrasil cell equipped with Mininert screw cap [polytetrafluoroethylene (PTFE)/silicone septa]. Because of the low solubility of  $FeCl_3$  in chloroform, aliquots of  $FeCl_3$  solution in acetonitrile were injected stepwise into the cell using an airtight microsyringe.

## RESULTS AND DISCUSSION

### Kinetics of Charge Attachment by Pulse Radiolysis.

High-energy radiation ejects electrons from THF and produces a solvated electron ( $e_s^-$ ) and a THF radical cation. Reduction of many aromatic molecules by solvated electrons [approximately  $-3.2$  V vs saturated calomel electrode (SCE)] occurs at diffusion-controlled rates, whereas deprotonation of THF cations<sup>41</sup> makes oxidation of solutes a minor process. Therefore, anions of many organic molecules are selectively produced, and their spectra and reactivities were studied by pulse radiolysis. Ionizing radiation of THF produces solvated electrons as the primary reducing species. Electrons attach to P3DT by fast processes described by



and the resulting  $P3DT^{\bullet-}$  species is stable over  $\gg 100$   $\mu$ s in THF.

A substantial fraction of the solvated electrons are geminate to positive counterions. Most geminate electrons disappear by recombination in  $\sim 1$  ns,<sup>42,43</sup> leaving a population of free ions having a lifetimes of a microsecond or more. Electron attachment over tens to hundreds of nanoseconds (Figure 2), therefore, creates principally free  $P3DT^{\bullet-}$  radical ions. From the observed decay of solvated electrons and the theory of geminate recombination,<sup>44,45</sup> one can expect that  $\sim 20\%$  of the electrons captured might be distant, long-lived geminate pairs, but these will produce  $P3DT^{\bullet-}$  ions that will combine with counterions only very slowly. The result is that, at (repeat-unit) concentrations of  $< 5$  mM, almost none the  $P3DT^{\bullet-}$  radical ions observed are in contact with counterions.

Hole attachment to P3DT was conducted in the chlorinated hydrocarbons chloroform and DCE. Hole transfer occurs from radiolytically generated solvent cations (reaction 2) and is slower than electron transfer from solvated electrons in THF (reaction 1) because of lower diffusion rates

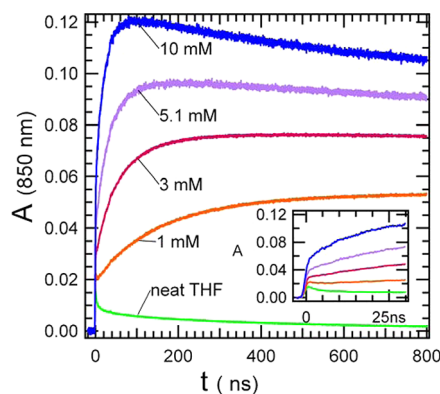
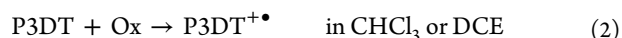


**Figure 2.** Transient absorption traces for electron attachment to P3DT in THF monitored at 850 nm at 1, 3, 5.1, and 10 mM (repeat-unit concentration). An expanded view in the inset shows more clearly the fast step formation of anions, apparently limited only by the  $\sim 2$ -ns detector response.



Radiolysis of chloroform is more complicated, and there seem to be at least two different species involved in oxidation,<sup>46–48</sup> but the identities of the oxidizing species have not been definitively established. Nevertheless, hole attachment to P3DT proceeds rapidly. P3DT cation formation was also studied in DCE, but aggregation and lower cation yields precluded quantitative measurements. Therefore, following hole attachment by pulse radiolysis was carried out in chloroform.

Transient absorption traces of reactions 1 and 2 showed nonexponential growth kinetics. Examples of these phenomena are presented in Figure 2 for different concentrations of P3DT monitored at 850 nm. Growth of  $T_4$  anion is shown in Figure S5 (Supporting Information), and its absorption spectrum is in Figures S6 and S7 (Supporting Information). The transient absorption in Figure 2 shows initial sudden rises, “steps”, limited by the detector response, followed by the more gradual diffusion-controlled growth processes. Four species can contribute to these steps: solvated electrons, singlet and triplet excited states of P3DT, and P3DT radical anions ( $P3DT^{\bullet-}$ ). Small yields of excited states are known to be formed in the pulse radiolysis of THF.<sup>49</sup> In the present experiments, emission was observed with a spectrum and lifetime of  $\sim 0.6$  ns similar to that reported for poly(3-octylthiophene) in THF.<sup>50</sup> For times longer than 2 ns, there are negligible contributions from singlets, which convert to triplets with a high quantum yield for intersystem crossing ( $\phi = 0.958$ ).<sup>50</sup> Contributions of solvated electrons were determined by measurements on neat THF. The absorption spectrum of the step in the range of 850–1600 nm, corrected for contributions from solvated electrons, resembles that of  $pT^{\bullet-}$ . The absorption spectrum of triplet states of polythiophene ( $\lambda_{max} = 800$ –850 nm) overlaps with the measured spectrum for the anion in this study. Their contribution was determined to be 5.8% of the maximum transient absorption by measuring the effect of 10 mM 2-ethylantraquinone (EtAQ), which was found to react rapidly with  $pT$  anions but not with  $pT$  triplets. At the highest concentration, 10 mM polymer repeat units (PRU),  $P3DT^{\bullet-}$  grows to a maximum at  $\sim 70$  ns. A substantial fraction, 24%, of this maximum is captured in the fast step process, similar to that reported recently for polyfluorenes.<sup>43</sup>



Fitting the slower growth process at 850 nm by a single exponential function yielded charge attachment rate constants of  $(9.0 \pm 1) \times 10^{11} \text{ M}^{-1} \text{ s}^{-1}$  for electrons in THF and  $(2.2 \pm 0.3) \times 10^{11} \text{ M}^{-1} \text{ s}^{-1}$  for holes in chloroform per polymer molecule using an average number of units of  $n = 170$ . Similar data in THF at 1000 nm, where solvated electrons absorb more strongly and triplets absorb little, were fitted with a kinetic model including solvated-electron decay and  $\text{P3DT}^{\bullet-}$  growth, a rate constant of  $(7.6 \pm 1) \times 10^{11} \text{ M}^{-1} \text{ s}^{-1}$  was obtained. The electron-attachment rate constants are about 10 times larger than attachment rates to small molecules such as biphenyl  $[(6.8\text{--}9.3) \times 10^{10} \text{ M}^{-1} \text{ s}^{-1}]$ , known to be at or near the diffusion-controlled limit.<sup>42,51,52</sup> This factor of  $\sim 10$  increase is in accord with theories for diffusion-controlled reaction rates to rod-shaped molecules by Traytak and Tsao.<sup>53–55</sup> These theories were applied by Grozema et al.<sup>17</sup> for hole transfer and by Takeda et al.<sup>33</sup> and Sreearunothai et al.<sup>52</sup> for electron transfer to polymers. The rates were not simply proportional to the length of the rod but scaled with  $n/(\ln n)$ , where  $n$  is the number of repeat units and the effective reaction radius is given by  $R_{\text{eff}} = nR_{\text{M}}/[1 + (2R_{\text{M}}/a)(\ln n)]$ . The present observations are in line with this prediction, and the relative reaction radius  $R_{\text{eff}}/R_{\text{M}}$  of 8 can be reproduced if the reaction radius for a monomer is twice the unit length of thiophene ( $R_{\text{M}} = 0.8 \text{ nm}$  if  $a = 0.4 \text{ nm}$ ). The rate constant of electron attachment to  $\text{T}_4$  ( $1.3 \times 10^{11} \text{ M}^{-1} \text{ s}^{-1}$ ) is also in accord with this picture, as is the kinetics, which depart from a single-exponential time dependence because of steric effects in diffusion-controlled reactions.<sup>17,33,52</sup>

**Absorption Spectra and Delocalization Lengths of Excess Charges.** The transient absorption spectrum of the P3DT anion in the range of 380–2500 nm 1  $\mu\text{s}$  after the electron pulse is presented in Figure 3 (solid circles). For the ranges of the neutral absorption bands and NIR bands, thinner cells and lower concentrations of polymer were used to enable

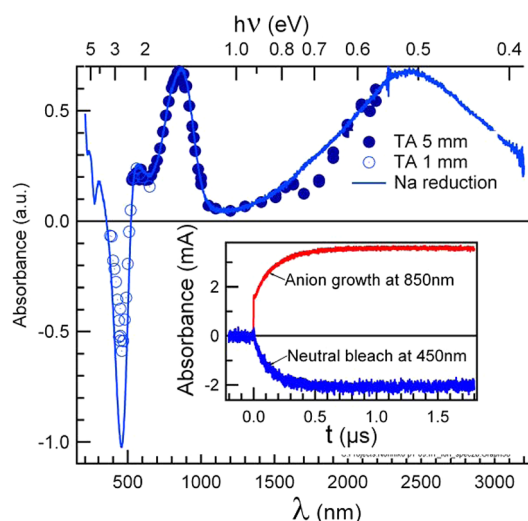


**Figure 3.** Transient absorption spectrum of P3DT anion produced by pulse radiolysis in THF. Spectra obtained in 3 mM (repeat-unit) solutions of P3DT in 5- and 1-mm cells were scaled to match the steady-state absorption spectrum obtained by reduction with sodium. The inset shows absorption traces obtained with a 1-mm cell monitored at 850 and 450 nm. The prompt step increase in absorption at 850 nm arises principally from absorption due to solvated electrons and prompt  $\text{P3DT}^{\bullet-}$  formation, with a smaller contribution from P3DT triplets (see text).

transmission of the probe light. Spectra from different data path lengths were scaled to each other to form a continuous spectrum in Figure 3. Upon electron attachment, the absorption bands at 850 nm (P2 band) and  $>1600 \text{ nm}$  (P1 band) grew, whereas the neutral band at 450 nm bleached. The spectrum obtained from pulse radiolysis matches fairly well with that of the early stages in sodium doping experiments (solid line), which will be discussed below.

The polaronic nature of the transient absorption spectrum in Figure 3 is required by the rapid charge injection and the higher concentration of P3DT (17  $\mu\text{M}$  P3DT molecule concentration based on  $n = 170$ ) compared to P3DT anions produced (1  $\mu\text{M}$ ). The 17:1 ratio makes it unlikely for more than one electron to attach to a P3DT molecule. Two P3DT molecules, each bearing one polaron, could meet to possibly form a bipolaron or a  $\pi$  dimer, but this process would require  $\sim 50 \mu\text{s}$  [for diffusion-controlled reactions,  $(\sim 2 \times 10^{10} \text{ M}^{-1} \text{ s}^{-1}) \times (\sim 1 \mu\text{M}) = \sim 2 \times 10^4 \text{ s}^{-1}$ ], much longer than the 950-ns time for the spectrum in Figure 3. Therefore, the spectrum in Figure 3 is due to single polarons,  $\text{P3DT}^{\bullet-}$ . By using biphenyl anion as the reference compound ( $\epsilon_{650} = 1.25 \times 10^4 \text{ M}^{-1} \text{ cm}^{-1}$ ),<sup>56–58</sup> yields and the absorption coefficient,  $\epsilon$ , of  $\text{P3DT}^{\bullet-}$  in the present pulse-radiolysis experiments were deduced. Using varied concentrations, we obtained  $\epsilon$  values for  $\text{P3DT}^{\bullet-}$  at 1000 and 850 nm as  $\epsilon_{1000} = (1.98 \pm 0.23) \times 10^4 \text{ M}^{-1} \text{ cm}^{-1}$  and  $\epsilon_{850} = (7.25 \pm 0.47) \times 10^4 \text{ M}^{-1} \text{ cm}^{-1}$ , respectively.

Similar experiments were performed with quaterthiophene,  $\text{T}_4$ , whose anions also had two principal absorption bands at 700 and 1300 nm. (See Figures S6 and S7 in the Supporting Information.) This procedure yielded  $\epsilon_{700} = (4.95 \pm 0.16) \times 10^4 \text{ M}^{-1} \text{ cm}^{-1}$  for  $\text{T}_4^{\bullet-}$ . Spectra of  $\text{T}_2^{\bullet-}$  and  $\text{T}_3^{\bullet-}$  were also obtained.

The absorption coefficient of neutral P3DT at 450 nm was measured to be  $8.3 \times 10^3 \text{ M}^{-1} \text{ cm}^{-1}$  per repeat unit. Simultaneous observation of growth of the anion band at 850 nm and the bleaching of neutral band at 450 nm for the same sample could tell how many monomer units were bleached when one charge was injected into a P3DT chain (Figure 3 inset). Quantitative assessment of the bleaching is complicated by the presence of an absorption band of the anion (P3 band) that overlaps the neutral band. If absorbance of the anion at 450 nm is estimated to be equal to that at the 570-nm origin of the P3DT neutral band, then  $9.5 \pm 1.2$  monomer units were bleached when one anion was injected into the chain. This procedure, similar to that described previously,<sup>33,59</sup> considers bleaching at a single wavelength, the maximum of the neutral band. A potentially better procedure adds back differing amounts of the neutral band to estimate the remaining anion. Results of this procedure shown in Figures S10 and S11 (Supporting Information) estimate that  $11.5 \pm 2.5$  repeat units are bleached when a single electron is injected (Figure 4). This corresponds to the spatial extent of 4.4 nm for the negative polaron. As found for polyfluorenes,<sup>33</sup> the spectra appear to contain only contributions from  $\text{P3DT}^{\bullet-}$  and P3DT neutral, aside from small contributions due to P3DT triplets. This observation is consistent with the interpretation that, upon electron injection, the electron exists as a  $\text{P3DT}^{\bullet-}$  polaron, located in a portion of the chain, whereas the remainder of the chain is neutral. The present work determined the delocalization length of the P3DT polaron by direct observation of optical spectra.

**Holes in P3DT.** Figure 5 shows the absorption spectra of holes injected into P3DT. The spectrum, with peaks for P2 and

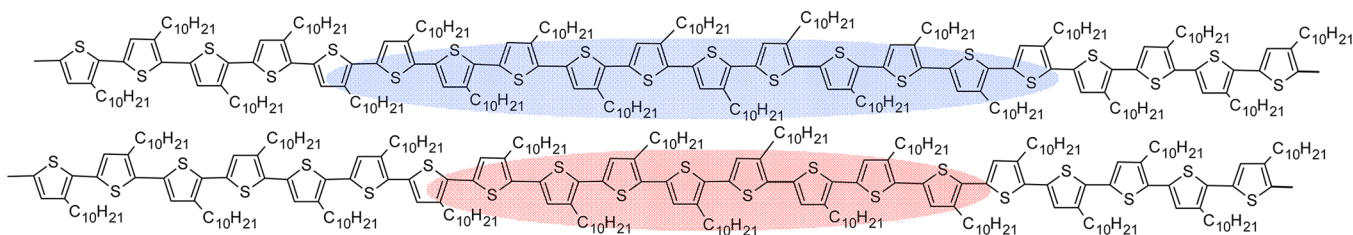


**Figure 4.** Spatial extents of (top) negative ( $\sim 11.5$  units) and (bottom) positive ( $\sim 8.7$  units) polarons estimated from pulse radiolysis.

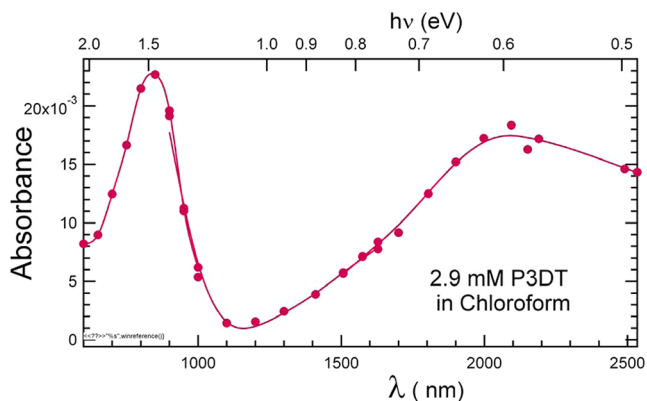


**Figure 5.** Transient absorption spectrum of P3DT cations produced by pulse radiolysis of 2.9 mM (monomer) P3DT in  $\text{CHCl}_3$ . The spectrum was recorded 500 ns after the pulse in a 5-mm cell.

P1 bands at 850 and 2100 nm, is similar to that of P3DT anions except for a slightly longer wavelength for the P1 band. It is not clear whether these holes are free ions or whether they are ion-paired with counterions because the chemistry following ionization of chloroform is only partly understood. The absorption coefficient of positive polarons was determined by charge transfer from the cation of the reference compound tritolyamine, TTA:  $\epsilon_{\text{TTA}^+} = 2.88 \times 10^4 \text{ M}^{-1} \text{ cm}^{-1}$  at 680 nm (Figure S12 in the Supporting Information).<sup>60,61</sup> The 680-nm absorption band of  $\text{TTA}^{+\bullet}$  is well separated from the visible band of  $\text{P3DT}^{+\bullet}$ . The absorption coefficient of the P3DT cation at 850 nm was determined to be  $(6.0 \pm 1) \times 10^4 \text{ M}^{-1} \text{ cm}^{-1}$  (after corrections for absorbance due to triplets noted in the Supporting Information). The concentration of P3DT cations in Figure 5 is, therefore,  $\sim 0.8 \mu\text{M}$ , which, as in the anion case, is much smaller than the  $17 \mu\text{M}$  concentration of P3DT polymer molecules. Procedures such as those depicted in Figures S10 and S11 (Supporting Information) for anions yielded 8.7 neutral thiophene units bleached upon the formation of one P3DT cation (Figure 4). The reaction with TTA did not go to completion, but formed an equilibrium,  $\text{TTA}^{+\bullet} + \text{P3DT} \rightleftharpoons \text{TTA} + \text{P3DT}^{+\bullet}$ . It was possible to roughly estimate the equilibrium constant,  $K_{\text{eq}} = 2600$ , uncertain by a factor of 2. With the redox potential for  $\text{TTA}^{+/0}$  of +0.23 V vs the ferrocenium/ferrocene redox couple ( $\text{Fc}^{+/0}$ ),<sup>39</sup> we estimated the  $E^0(\text{P3DT}^{+/0}) = +0.03 \pm 0.02 \text{ V}$  vs  $\text{Fc}^{+/0}$  for adding one hole to P3DT. The uncertainty here does not include that due to uncertainty about ion pairing. If the ions observed here are paired, the pairing would be likely to stabilize the TTA cation by a few hundred millielectronvolts but would stabilize P3DT cations by a smaller amount. This would effectively make  $K_{\text{eq}}$  smaller and  $E^0(\text{P3DT}^{+/0})$  more positive. Potentials for oxidation of series of alkylated oligothiophene,  $\text{T}_n$ , measured by cyclic voltammetry vs  $\text{Fc}^{+/0}$  become less

positive with increasing number of units  $n$  and approach the value of  $E^0(\text{P3DT}^{+/0})$  estimated above;  $E^0 = 0.51, 0.34, 0.19$ , and  $0.12$  ( $n = 4, 8, 12, 16$ , respectively) in DCE by Bauerle et al.<sup>62</sup> and  $E^0 = 0.34, 0.15$ , and  $0.12$  ( $n = 6, 9, 12$ ) in  $\text{CH}_2\text{Cl}_2$  by van Haare et al.<sup>63</sup> This trend of  $E^0$  versus  $1/n$  is also consistent with similar potentials for  $\text{T}_n$  in  $\text{CH}_2\text{Cl}_2$  from Meerholz and Heinze,<sup>64</sup> who extrapolated to  $-0.03 \text{ V}$  for polythiophene.<sup>65,66</sup>

On the other hand, chemical oxidation in chloroform using  $\text{FeCl}_3$  (Figure S13, Supporting Information) produced different band shapes and positions from the radiolytically generated cations, most notably an additional band at 590 nm (2.1 eV). This might suggest that chloride ions (or  $\text{FeCl}_4^-$ ) bind strongly to  $\text{P3DT}^{+\bullet}$  in chloroform. Whereas Fratiloiu et al. attributed changes in chemically produced spectra for fluorene-based polymers in  $\text{CCl}_4$  to interactions of multiple charges,<sup>67</sup> van Haare et al.<sup>63</sup> did not observe such a band upon adding 2 oxidizing equivalents to  $\text{T}_{12}$ . Spectra of cations produced by  $\text{FeCl}_3$  in DCE showed peaks at  $\sim 800$  and  $\sim 2200 \text{ nm}$ , closer to what may be “free” cations produced by pulse radiolysis in  $\text{CHCl}_3$ . The higher polarity of DCE would be expected to reduce ion-pairing. However, the conformation of P3DT seems different in DCE since significant broadening and appearance of multiple peaks were found in neutral absorption spectra (Figure S3, Supporting Information).

**Comparison with Oligomers and Other Studies.** The absorption spectra for  $\text{P3DT}^{+\bullet}$  and  $\text{P3DT}^{+\bullet}$  are similar (Figures 3 and 5) and the delocalization lengths for negative ( $\sim 11.5$  units, 4.6 nm) and positive polarons ( $\sim 8.7$  units, 3.5 nm) are not very different (Figure 4). These lengths are similar to those deduced for anions of polyfluorene or oligofluorenes in THF solution<sup>33,68</sup> and to data from long oligomers described below. The transition energies of series of oligothiophene ions decrease with increasing number of thiophene units with more delocalized charges. Figure 6 shows transient absorption of  $\text{T}_n^{+\bullet}$  ( $n = 2-4$ ), and Figure 7 compares energies for the P1 and

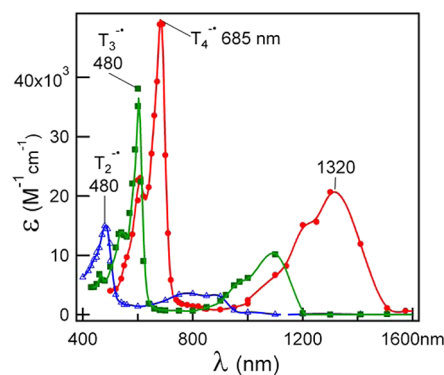


**Figure 6.** Absorption spectra of radical anions of oligothiophenes,  $\text{T}_n^{+\bullet}$  ( $n = 2-4$ ), in THF measured by pulse radiolysis.

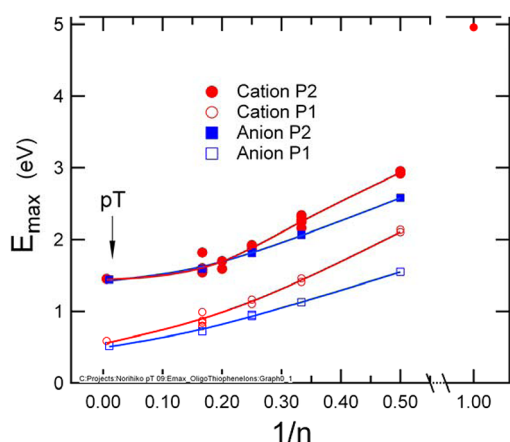


**Figure 7.** Peak energies of near-IR (P1) and UV-visible (P2) absorption bands for monoanions and cations of oligothiophenes,  $T_n$ , reported in the literature,<sup>69–82</sup> along with results from this study. Results reported herein for P3DT anion and cation are included with  $n = 170$ .

P2 bands of anions  $T_n^{\bullet-}$ ,  $n = 2–4$ , with Baurele's<sup>69</sup>  $T_6$  and with extensive results on  $T_n^{+\bullet}$  from the literature<sup>69–82</sup> as well as the present results for polarons in polythiophenes.

For long molecules like polythiophene studied here, the electronic coupling tends to delocalize a charge over entire molecule while electron–phonon coupling tends to localize it to a shorter length. The latter effect is accompanied by structural deformation around the charge to stabilize ionized molecule. The position of intragap states is influenced by structural deformation and reflected in the transition energies.<sup>8</sup> From the plots of transition energies of  $T_n$  cations against  $1/n$  and comparisons with polythiophene cations, a delocalization length of positive polaron  $n \approx 12$  was deduced.<sup>80,83–85</sup> van Haare et al.<sup>63</sup> oxidized  $T_6$ ,  $T_9$ ,  $T_{12}$  and observed shift of absorption spectra from  $T_6^{+\bullet}$  to  $T_9^{+\bullet}$  to  $T_{12}^{+\bullet}$ . Therefore, delocalization is considered to be  $n > 9$ . For anions, absorption spectra with  $n > 6$  are not available but  $T_2$  to  $T_6$  cations show similar trends with slightly red-shifted spectra. The present results also fall on these trends found in the literature. The delocalization length estimated here for  $P3DT^{\bullet-}$  in solution is comparable to the value  $n \approx 10$  deduced from spin densities in LENDOR studies<sup>86,87</sup> for  $P3DT^{+\bullet}$  at low temperature in a solvent-free environment.

We performed molecular orbital calculations on series of oligothiophenes (in vacuum) to see if the delocalization length of negative polaron determined experimentally here is supported by computation. However, the degree of charge delocalization in long oligothiophenes was greatly influenced by the computational methods used. The delocalization length of negative polaron  $P3DT^{\bullet-}$  determined here ( $\sim 11.5$  units) falls between computational estimates of delocalization length for  $P3DT^{\bullet-}$  from semiempirical and DFT methods (see Figures S14–S17 in the Supporting Information). Similar effects were also reported previously for oligothiophene cations<sup>88</sup> Apart from variation by different computational methods, the delocalization length of polarons in real molecules could be limited by conformation changes of polymers by thermal fluctuations and solvation (e.g., rotation around inter-ring bond), charge compensation by counterion, and by structural defects.

**Multiple Polarons in a Single Chain.** From the above estimation of the delocalization length of single polarons ( $L_p$ )

in P3DT, it is possible to store multiple polarons in a single polythiophene chain with its length much longer than  $L_p$ . In the study of oxidation of  $T_{12}$ , the possibility of multiple positive polarons was discussed.<sup>63</sup> Previously, relative thermodynamic stabilities of polarons versus bipolarons were found to favor bipolarons.<sup>8,9,29</sup> If this is the case, when multiple charges are injected to a long molecule like polythiophene, for example by chemical reduction with sodium, it would show different spectral signatures from those of polarons. On the contrary, the present paper reports optical absorption spectra of chemically reduced P3DT very similar to those of  $P3DT^{\bullet-}$  single polaron observed by pulse radiolysis. The UV–vis–NIR absorption spectra of chemically reduced P3DT in THF are shown in Figure 8. The spectrum measured before contacting sodium

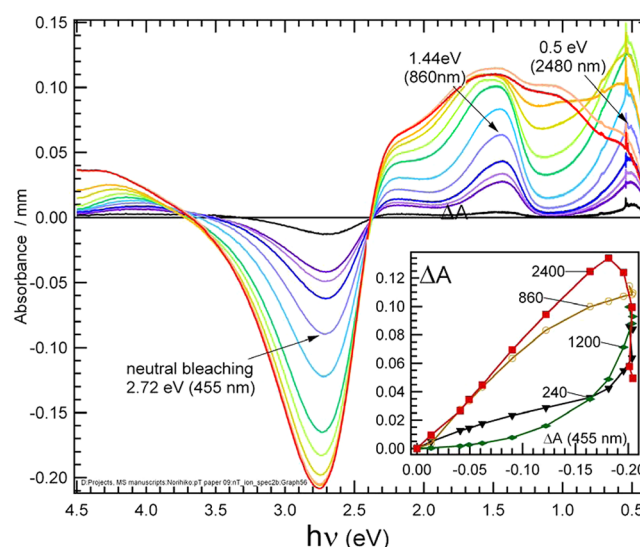


**Figure 8.** Chemical reduction of P3DT by sodium in THF, indicating the formation of multiple polarons in a single chain. The optical absorption data, in a 1-mm-path-length cell, are presented as difference spectra relative to the neutral. The inset shows difference changes with reduction as a function of the absorbance change at 455 nm.

film was subtracted from successively measured spectra. By utilizing a short optical length (1 mm), reasonably good spectra could be obtained in spite of solvent absorption bands in the near IR region. Upon contacting with sodium, bleaching of the neutral band is observed which was accompanied by growth of two absorption bands at  $\sim 860$  nm (1.44 eV) and  $\sim 2400$  nm (0.52 eV). The absorbance of these new bands are nearly identical and grow linearly with the decrease of the neutral peak at 450 nm (Figure 8 inset) and isosbestic points were found at  $\sim 340$  and  $\sim 520$  nm. Therefore, the two new absorption bands in visible and near IR regions can be assigned to P3DT anions formed by reactions with sodium (P2 and P1). The early stages of the spectra are similar to those of free anion produced by pulse radiolysis, suggesting that sodium counterion has little effect on the polarons, or at least on their optical spectra. There seems to be an anion absorption band extending into UV region overlapping with the neutral band (P3). While overlap of absorption bands occurs, as seen above, the measured bleaching of neutral absorption is significantly larger than observed in the pulse-radiolysis experiment. The transient spectrum obtained by pulse radiolysis is likely to be more reliable because complications from the side reactions, including disproportionation<sup>63</sup> and adsorption on the surface



is less likely. Assuming all of the neutral segment is converted to anions after the bleaching at 450 nm has leveled off, the extent of neutral bleaching is underestimated by 27% if the peak absorbance change seen in Figure 8 is considered. Anion bands became broader as more than about half of the neutral band was bleached. Concomitantly, the ratio of intensities of 2400 nm band to that of 860 nm became greater and approached about 1.3. However, the overall spectral shape did not change significantly until the bleaching of the neutral band started to level off. After that a 2400 nm band declined and a new band at around 1200 nm emerged. At this stage the anion band in vis–NIR region seems more like a one broad band with three peaks.

The estimation of number of anion species produced in each step of reduction is not possible by the present experiments alone since quantitative measure of reacted sodium is difficult. Furthermore it is probable that side reactions and adsorption of reduced P3DT on sodium film surface could compromise quantitative determinations. Similar reductions of  $T_4$  by Na (Figures S8 and S9, Supporting Information) point to complexities at early stages. However by using the absorption coefficient of one-electron reduced P3DT derived from pulse radiolysis (described above), it can be estimated that at least 8 electrons were injected per one polymer chain of average length ( $n \approx 170$ ) before significantly changing the spectral shape. The present results suggest that multiple polarons can be stored in a single P3DT chain. While the results do not exclude the presence of other forms such as bipolarons, clearly several polarons can coexist on a chain, consistent with the observations of van Haare et al. on oligomers.<sup>63</sup>

Early work<sup>89</sup> noted that sodium doping of polythiophene creates intragap states 0.65–0.7 eV below the conduction-band edge and 0.6–0.65 eV above the valence-band edge assigned to bipolarons, and spectroelectrochemical studies reported two similar absorption bands at 1.5–1.8 and 0.6–0.7 eV for reduced polythiophene films although relative magnitudes and exact peak positions differ.<sup>2,90</sup> Other works reported part of the spectrum for polythiophene films<sup>91,92</sup> which are in a rough agreement with our results. Figures 3 and 8 present a full UV–vis–NIR spectra of reduced polythiophene in solution for the first time. The slight differences in peak position from different authors could be due to different degree of conjugation among different samples (defects, morphologies) and different environment.

The spectral changes observed in Figure 8 upon further doping are indicative of a transition from monoion (polaron) to diion (bipolaron).<sup>10,28,93–95</sup> Alternatively, upon injection of multiple charges into a single chain, Coulombic repulsions between neighboring polarons could localize each polaron, thus change the orbital energies (array of polaron). The identification of spectroscopic features of later stages of reduced P3DT in Figure 8 as either a bipolaron or polaron array is not clear from information reported here.

## CONCLUSIONS

The optical absorption spectra of  $P3DT^{\bullet-}$  and  $P3DT^{++}$ , definitely identified as polarons in P3DT, contain a strong near-infrared P1 band and a higher-energy P2 band similar to those known for delocalized electrons or holes in other conjugated polymers. Extinction coefficients were determined for the absorption bands of  $P3DT^{\bullet-}$  and less accurate ones for those of  $P3DT^{++}$ . The electron in  $P3DT^{\bullet-}$  was determined to be delocalized over  $\sim 11.5$  repeat units, whereas the hole was estimated to be delocalized over  $\sim 8.7$  repeat units. Although

the difference could reflect fundamental properties of the polarons,  $P3DT^{\bullet-}$  radical ions in THF are free ions, whereas possible ion pairing of  $P3DT^{++}$  in chloroform is not known. The absorption bands were also utilized to determine kinetics of charge attachment.

The kinetics of attachment of solvated electrons to P3DT showed time-dependent rates due to transient effects for long molecules and, at moderately large concentrations, also showed the sudden formation of anions due to fast step electron capture that occurs prior to diffusion of the solvated electrons. These step processes give very fast ( $< 2$ -ns) formation of  $P3DT^{\bullet-}$  and could enable examination of polarons and their transport with high time resolution.

Chemical reduction (doping) by Na metal was compared with the results from pulse radiolysis. Although the experiments do not give quantitative determination of the numbers of anions, the shapes of the spectra in early stages of reduction are very similar to those definitively identified as  $P3DT^{\bullet-}$  polarons. Results of oxidative doping by  $FeCl_3$  also appear to give polarons in the early stages. These results indicate that multiple polarons can exist in a single chain of polythiophene in solution.

## ASSOCIATED CONTENT

### Supporting Information

GPC trace of P3DT, optical absorption spectra of neutral poly- and oligothiophenes, graphical representations of procedures for estimating the number of bleached neutral thiophene units from transient absorption spectrum of P3DT anion, additional data on quaterthiophene anions in THF and P3DT cations in chloroform, and molecular orbital calculation results of model oligothiophenes ( $T_n$ ). This material is available free of charge via the Internet at <http://pubs.acs.org>.

## AUTHOR INFORMATION

### Corresponding Author

\*E-mail: [jrmiller@bnl.gov](mailto:jrmiller@bnl.gov).

### Notes

The authors declare no competing financial interest.

## ACKNOWLEDGMENTS

The authors gratefully acknowledge support from the Division of Chemical Sciences, Geosciences, and Biosciences, Office of Basic Energy Sciences, U.S. Department of Energy, through Grant DE-AC02-98-CH10886 and use of the LEAF Facility of the BNL Accelerator Center for Energy Research.

## REFERENCES

- (1) Chung, T. C.; Kaufman, J. H.; Heeger, A. J.; Wudl, F. *Phys. Rev. B* **1984**, *30*, 702–710.
- (2) Kaneto, K.; Kohno, Y.; Yoshino, K. *Solid State Commun.* **1984**, *51*, 267–269.
- (3) Yoshino, K.; Hayashi, S.; Kohno, Y.; Kaneto, K.; Okube, J.; Moriya, T. *Jpn. J. Appl. Phys., Part 2* **1984**, *23*, L198–L200.
- (4) Li, G.; Shrotriya, V.; Huang, J. S.; Yao, Y.; Moriarty, T.; Emery, K.; Yang, Y. *Nat. Mater.* **2005**, *4*, 864–868.
- (5) Su, W. P.; Schrieffer, J. R.; Heeger, A. J. *Phys. Rev. B* **1980**, *22*, 2099–2111.
- (6) Brazovskii, S. A.; Kirova, N. N. *JETP Lett.* **1981**, *33*, 4–8.
- (7) Fesser, K.; Bishop, A. R.; Campbell, D. K. *Phys. Rev. B* **1983**, *27*, 4804–4825.
- (8) Bredas, J. L.; Street, G. B. *Acc. Chem. Res.* **1985**, *18*, 309–315.
- (9) Harbecke, G.; Baeriswyl, D.; Kiess, H.; Kobel, W. *Phys. Scr.* **1986**, *T13*, 302–305.

- (10) Nowak, M. J.; Rughooputh, S.; Hotta, S.; Heeger, A. J. *Macromolecules* **1987**, *20*, 965–968.
- (11) Furukawa, Y. *J. Phys. Chem.* **1996**, *100*, 15644–15653.
- (12) Zamoshchik, N.; Bendikov, M. *Adv. Funct. Mater.* **2008**, *18*, 3377–3385.
- (13) Zade, S. S.; Zamoshchik, N.; Bendikov, M. *Acc. Chem. Res.* **2011**, *44*, 14–24.
- (14) Zade, S. S.; Bendikov, M. *J. Phys. Chem. B* **2006**, *110*, 15839–15846.
- (15) Salzner, U. *J. Phys. Chem. A* **2008**, *112*, 5458–5466.
- (16) Alkan, F.; Salzner, U. *J. Phys. Chem. A* **2008**, *112*, 6053–6058.
- (17) Grozema, F. C.; Hoofman, R.; Candeias, L. P.; de Haas, M. P.; Warman, J. M.; Siebbeles, L. D. A. *J. Phys. Chem. A* **2003**, *107*, 5976–5986.
- (18) Prins, P.; Grozema, F. C.; Schins, J. M.; Patil, S.; Scherf, U.; Siebbeles, L. D. A. *Phys. Rev. Lett.* **2006**, *96*.
- (19) Grozema, F. C.; Warman, J. M. *Radiat. Phys. Chem.* **2005**, *74*, 234–238.
- (20) Dicker, G.; de Haas, M. P.; Warman, J. M.; de Leeuw, D. M.; Siebbeles, L. D. A. *J. Phys. Chem. B* **2004**, *108*, 17818–17824.
- (21) Grozema, F. C.; Siebbeles, L. D. A.; Warman, J. M.; Seki, S.; Tagawa, S.; Scherf, U. *Adv. Mater. Processes* **2002**, *14*, 228–231.
- (22) Warman, J. M.; Gelinck, G. H.; Piet, J. J.; Suykerbuyk, J. W. A.; De Haas, M. P.; Langeveld-Voss, B. M. W.; Janssen, R. A. J.; Hwang, D.-H.; Holmes, A. B.; Remmers, M.; Neher, D.; Müllen, K.; Bäuerle, P. *Proc. SPIE* **1997**, *3145*, 142–149.
- (23) Saeki, A.; Ohsaki, S.-i.; Seki, S.; Tagawa, S. *J. Phys. Chem. C* **2008**, *112*, 16643–16650.
- (24) Yagai, S.; Kinoshita, T.; Kikkawa, Y.; Karatsu, T.; Kitamura, A.; Honsho, Y.; Seki, S. *Chem.—Eur. J.* **2009**, *15*, 9320–9324.
- (25) Ohnishi, Y.; Saeki, A.; Seki, S.; Tagawa, S. *J. Chem. Phys.* **2009**, *130*.
- (26) Sugiyasu, K.; Honsho, Y.; Harrison, R. M.; Sato, A.; Yasuda, T.; Seki, S.; Takeuchi, M. *J. Am. Chem. Soc.* **2010**, *132*, 14754–14756.
- (27) Saeki, A.; Koizumi, Y.; Aida, T.; Seki, S. *Acc. Chem. Res.* **2012**, *45*, 1193–1202.
- (28) Nowak, M. J.; Spiegel, D.; Hotta, S.; Heeger, A. J.; Pincus, P. A. *Macromolecules* **1989**, *22*, 2917–2926.
- (29) Colaneri, N.; Nowak, M.; Spiegel, D.; Hotta, S.; Heeger, A. J. *Phys. Rev. B* **1987**, *36*, 7964–7968.
- (30) Yokonuma, N.; Furukawa, Y.; Tasumi, M.; Kuroda, M.; Nakayama, J. *Chem. Phys. Lett.* **1996**, *255*, 431–436.
- (31) Gonzalez, S. R.; Ie, Y.; Aso, Y.; Navarrete, J. T. L.; Casado, J. J. *Am. Chem. Soc.* **2011**, *133*, 16350–16353.
- (32) Chen, X. W.; Inganas, O. *J. Phys. Chem.* **1996**, *100*, 15202–15206.
- (33) Takeda, N.; Asaoka, S.; Miller, J. R. *J. Am. Chem. Soc.* **2006**, *128*, 16073–16082.
- (34) Chen, T. A.; Wu, X. M.; Rieke, R. D. *J. Am. Chem. Soc.* **1995**, *117*, 233–244.
- (35) Katz, H. E.; Torsi, L.; Dodabalapur, A. *Chem. Mater.* **1995**, *7*, 2235–37.
- (36) Wishart, J. F. In *Radiation Chemistry: Present Status and Future Trends*; Jonah, C. D., Rao, B. S. M., Eds.; Elsevier Science: Amsterdam, 2001; Vol. 87, pp 21–35.
- (37) Wishart, J. F.; Cook, A. R.; Miller, J. R. *Rev. Sci. Instrum.* **2004**, *75*, 4359–4366.
- (38) Miller, J. R.; Penfield, K.; Johnson, M.; Closs, G.; Green, N. In *Photochemistry and Radiation Chemistry. Complementary Methods for the Study of Electron Transfer*; Wishart, J. F., Nocera, D. G., Eds.; American Chemical Society: Washington, DC, 1998; Vol. 254, pp 161–176.
- (39) Asaoka, S.; Takeda, N.; Iyoda, T.; Cook, A. R.; Miller, J. R. *J. Am. Chem. Soc.* **2008**, *130*, 11912–11920.
- (40) Rumbles, G.; Samuel, I. D. W.; Magnani, L.; Murray, K. A.; DeMello, A. J.; Crystall, B.; Moratti, S. C.; Stone, B. M.; Holmes, A. B.; Friend, R. H. *Synth. Met.* **1996**, *76*, 47–51.
- (41) Tranthi, T. H.; Koulkes-Pujo, A. M. *J. Phys. Chem.* **1983**, *87*, 1166–1169.
- (42) De Waele, V.; Sorgues, S.; Pernot, P.; Marignier, J. L.; Monard, H.; Larbre, J. P.; Mostafavi, M. *Chem. Phys. Lett.* **2006**, *423*, 30–34.
- (43) Cook, A. R.; Sreearunothai, P.; Asaoka, S.; Miller, J. R. *J. Phys. Chem. A* **2011**, *115*, 11615–11623.
- (44) Hong, K. M.; Noolandi, J. *J. Chem. Phys.* **1978**, *68*, 5163–5171.
- (45) Vandenende, C. A. M.; Luthjens, L. H.; Warman, J. M.; Hummel, A. *Radiat. Phys. Chem.* **1982**, *19*, 455–466.
- (46) Buhler, R. E. *J. Radioanal. Nucl. Chem.* **1986**, *101*, 329–338.
- (47) Washio, M.; Tagawa, S.; Furuya, K.; Hayashi, N.; Tabata, Y. *Radiat. Phys. Chem.* **1989**, *34*, 533–537.
- (48) Washio, M.; Yoshida, Y.; Hayashi, N.; Kobayashi, H.; Tagawa, S.; Tabata, Y. *Radiat. Phys. Chem.* **1989**, *34*, 115–120.
- (49) Kemp, T. J.; Roberts, J. P. *Trans. Faraday Soc.* **1968**, *64*, 2106–&.
- (50) Kodaira, T.; Watanabe, A.; Ito, O.; Watanabe, M.; Saito, H.; Koishi, M. *J. Phys. Chem.* **1996**, *100*, 15309–15313.
- (51) Saeki, A.; Kozawa, T.; Ohnishi, Y.; Tagawa, S. *J. Phys. Chem. A* **2007**, *111*, 1229–1235.
- (52) Sreearunothai, P.; Asaoka, S.; Cook, A. R.; Miller, J. R. *J. Phys. Chem. A* **2009**, *113*, 2786–2795.
- (53) Traytak, S. D. *Chem. Phys. Lett.* **1992**, *197*, 247–254.
- (54) Traytak, S. D. *Chem. Phys. Lett.* **1994**, *227*, 180–186.
- (55) Tsao, H. K.; Lu, S. Y.; Tseng, C. Y. *J. Chem. Phys.* **2001**, *115*, 3827–3833.
- (56) Balk, P.; Debruijn, S.; Hoijtink, G. J. *Recl. Trav. Chim. Pays-Bas* **1957**, *76*, 907–918.
- (57) Balk, P.; Hoijtink, G. J.; Schreurs, J. W. H. *Recl. Trav. Chim. Pays-Bas* **1957**, *76*, 813–823.
- (58) Jagur-Grodzinski, J.; Feld, M.; Yang, S. L.; Szwarc, M. *J. Phys. Chem.* **1965**, *69*, 628–35.
- (59) Seki, S.; Yoshida, Y.; Tagawa, S. *Radiat. Phys. Chem.* **2001**, *60*, 411–415.
- (60) Pedersen, L.; Pedersen, S. U. Aarhus Univ, Aarhus, Denmark. Private communication, 2007.
- (61) Pedersen, S. U.; Christensen, T. B.; Thomasen, T.; Daasbjerg, K. *J. Electroanal. Chem.* **1998**, *454*, 123–143.
- (62) Bauerle, P.; Fischer, T.; Bidlingmeier, B.; Stabel, A.; Rabe, J. P. *Angew. Chem., Int. Ed. Engl.* **1995**, *34*, 303–307.
- (63) van Haare, J.; Havinga, E. E.; van Dongen, J. L. J.; Janssen, R. A. J.; Cornil, J.; Bredas, J. L. *Chem.—Eur. J.* **1998**, *4*, 1509–1522.
- (64) Meerholz, K.; Heinze, J. *Electrochim. Acta* **1996**, *41*, 1839–1854.
- (65) These potentials versus Ag/AgCl use an approximate correction to Fc based on  $E^0(\text{Fc}^{+/0}) = +0.38$  V reported in ref 66.
- (66) Smie, A.; Synowczyk, A.; Heinze, J.; Alle, R.; Tschuncky, P.; Gotz, G.; Bauerle, P. *J. Electroanal. Chem.* **1998**, *452*, 87–95.
- (67) Fratiloin, S.; Fonseca, S. M.; Grozema, F. C.; Burrows, H. D.; Costa, M. L.; Charas, A.; Morgado, J.; Siebbeles, L. D. A. *J. Phys. Chem. C* **2007**, *111*, 5812–5820.
- (68) Zaikowski, L.; Kaur, P.; Gelfond, C.; Selvaggio, E.; Asaoka, S.; Wu, Q.; Chen, H. C.; Takeda, N.; Cook, A. R.; Yang, A.; Cook, A. R.; Yang, A.; Rosanelli, J.; Miller, J. R. *J. Am. Chem. Soc.* **2012**, *134*, 10852–10863.
- (69) Bauerle, P.; Segelbacher, U.; Gaudl, K. U.; Huttenlocher, D.; Mehrling, M. *Angew. Chem., Int. Ed. Engl.* **1993**, *32*, 76–78.
- (70) Garcia, P.; Pernaut, J. M.; Hapiot, P.; Wintgens, V.; Valat, P.; Garnier, F.; Delabouglise, D. *J. Phys. Chem.* **1993**, *97*, 513–516.
- (71) Wintgens, V.; Valat, P.; Garnier, F. *J. Phys. Chem.* **1994**, *98*, 228–232.
- (72) Poplawski, J.; Ehrenfreund, E.; Cornil, J.; Bredas, J. L.; Pugh, R.; Ibrahim, M.; Frank, A. J. *Synth. Met.* **1995**, *69*, 401–402.
- (73) Poplawski, J.; Ehrenfreund, E.; Cornil, J.; Bredas, J. L.; Pugh, R.; Ibrahim, M.; Frank, A. J. *Mol. Cryst. Liq. Cryst. Sci. Technol. A* **1994**, *256*, 407–413.
- (74) Keszthelyi, T.; Grage, M. M. L.; Offersgaard, J. F.; Wilbrandt, R.; Svendsen, C.; Mortensen, O. S.; Pedersen, J. K.; Jensen, H. J. A. *J. Phys. Chem. A* **2000**, *104*, 2808–2823.
- (75) Bauerle, P.; Segelbacher, U.; Maier, A.; Mehrling, M. *J. Am. Chem. Soc.* **1993**, *115*, 10217–10223.



- (76) Scaiano, J. C.; Evans, C.; Arnason, J. T. *J. Photochem. Photobiol. B* **1989**, *3*, 411–418.
- (77) Evans, C. H.; Scaiano, J. C. *J. Am. Chem. Soc.* **1990**, *112*, 2694–2701.
- (78) Emmi, S. S.; D'Angelantonio, M.; Poggi, G.; Beggiato, G.; Camaioni, N.; Geri, A.; Martelli, A.; Pietropaolo, D.; Zotti, G. *Res. Chem. Intermed.* **1998**, *24*, 1–14.
- (79) Emmi, S. S.; D'Angelantonio, M.; Beggiato, G.; Poggi, G.; Geri, A.; Pietropaolo, D.; Zotti, G. *Radiat. Phys. Chem.* **1999**, *54*, 263–270.
- (80) Guay, J.; Kasai, P.; Diaz, A.; Wu, R. L.; Tour, J. M.; Dao, L. H. *Chem. Mater.* **1992**, *4*, 1097–1105.
- (81) Fichou, D.; Horowitz, G.; Garnier, F. *Synth. Met.* **1990**, *39*, 125–131.
- (82) Caspar, J. V.; Ramamurthy, V.; Corbin, D. R. *J. Am. Chem. Soc.* **1991**, *113*, 600–610.
- (83) Guay, J.; Diaz, A.; Wu, R. L.; Tour, J. M.; Dao, L. H. *Chem. Mater.* **1992**, *4*, 254–255.
- (84) Guay, J.; Diaz, A.; Wu, R. L.; Tour, J. M. *J. Am. Chem. Soc.* **1993**, *115*, 1869–1874.
- (85) Diers, J. R.; Dearmond, M. K.; Guay, J.; Diaz, A.; Wu, R. L.; Schumm, J. S.; Tour, J. M. *Chem. Mater.* **1994**, *6*, 327–332.
- (86) Kuroda, S.; Marumoto, K.; Sakanaka, T.; Takeuchi, N.; Shimoi, Y.; Abe, S.; Kokubo, H.; Yamamoto, T. *Chem. Phys. Lett.* **2007**, *435*, 273–277.
- (87) Marumoto, K.; Takeuchi, N.; Kuroda, S. *Chem. Phys. Lett.* **2003**, *382*, 541–546.
- (88) Geskin, V. M.; Bredas, J. L. *Int. J. Quantum Chem.* **2003**, *91*, 303–310.
- (89) Bredas, J. L.; Themans, B.; Fripiat, J. G.; Andre, J. M.; Chance, R. R. *Phys. Rev. B* **1984**, *29*, 6761–6773.
- (90) Kaneto, K.; Ura, S.; Yoshino, K.; Inuishi, Y. *Jpn. J. Appl. Phys., Part 2* **1984**, *23*, L189–L191.
- (91) Crooks, R. M.; Chyan, O. M. R.; Wrighton, M. S. *Chem. Mater.* **1989**, *1*, 2–4.
- (92) Kvarnstrom, C.; Neugebauer, H.; Ivaska, A.; Sariciftci, N. S. *J. Mol. Struct.* **2000**, *521*, 271–277.
- (93) Rughooputh, S. D.; Fite, C. *Mol. Cryst. Liq. Cryst. Sci. Technol. A* **1993**, *231*, 215–222.
- (94) Hoier, S. N.; Park, S. M. *J. Phys. Chem.* **1992**, *96*, 5188–5193.
- (95) Zotti, G.; Schiavon, G.; Berlin, A.; Pagani, G. *Chem. Mater.* **1993**, *5*, 620–624.